

*Letter to the Editor***The origin of the HH 7–11 outflow*****R. Bachiller¹, F. Gueth², S. Guilloteau³, M. Tafalla¹, and A. Dutrey³**¹ IGN Observatorio Astronómico Nacional, Apartado 1143, 28800 Alcalá de Henares, Spain (bachiller@oan.es)² Max-Planck-Institut für Radioastronomie, Auf dem Hügel 69, 53121 Bonn, Germany³ Institut de Radio Astronomie Millimétrique, 300 rue de la Piscine, 38406 Saint Martin d'Hères, France

Received 15 August 2000 / Accepted 26 September 2000

Abstract. New, high-sensitivity interferometric CO $J=2-1$ observations of the HH 7–11 outflow show that despite previous doubts, this system is powered by the Class I source SVS 13. The molecular outflow from SVS 13 is formed by a shell with a large opening angle at the base, which is typical of outflows from Class I sources, but it also contains an extremely-high-velocity jet composed of “molecular bullets”, which is more typical of Class 0 outflows. This suggests that SVS 13 could be a very young Class I, which still keeps some features of the previous evolutionary stage. We briefly discuss the nature of some sources in the SVS 13 vicinity which are emitters of cm-wave continuum, but have no counterpart at mm wavelengths.

Key words: stars: formation – ISM: individual objects: HH7–11, NGC1333 – ISM: jets and outflows – ISM: molecules

1. Introduction

HH 7–11 is one of the most conspicuous chains of Herbig-Haro (HH) objects. It lies $\sim 6'$ South from NGC1333, in a region crowded of young stellar objects (YSOs) and low-mass star-formation signposts (bright and dark nebulosities, jets, OH and water masers, etc.). The region is at only ~ 300 pc from the Sun (Herbig & Jones 1983, Cernis 1992). Overall views in the optical and the infrared have been reported by Aspin et al. (1994), Hodapp & Ladd (1995) and Bally et al. (1996).

HH 7–11 is the optically visible part of an energetic high-velocity outflow which has bright emission in CO (Snell & Edwards 1981, Bachiller & Cernicharo 1990, Masson et al. 1990, Knee & Sandell 2000), H₂ (Hodapp & Ladd 1995), HI (Lizano et al. 1988, Rodríguez et al. 1990), and SiO (Lefloch et al. 1998, Codella et al. 1999). In spite of so many detailed studies, the HH 7–11 area is so rich in YSOs that identifying the outflow driving source is not an easy task. For as long as 20 years the infrared star SVS 13 (Strom et al. 1976), which is approximately

aligned with the HH 7–11 string, was believed to be its exciting source. However, recent radio observations (Rodríguez et al. 1997, 1999) have revealed new radio sources close to SVS 13 and have casted doubts about which is the source actually driving the outflow. Rodríguez et al. (1997) and Anglada et al. (2000) favored VLA 3, a source placed $6''$ SW from SVS 13 and also well aligned with the HH 7–11 chain, as the most likely exciting source of the outflow. The region is made even more complex by the presence of two other nearby sources, the radio source VLA 20 (Rodríguez et al. 1999) and the Class 0 protostar SVS 13B (Bachiller et al. 1998). The latter is known to drive a highly collimated SiO jet (Bachiller et al. 1998). We report interferometric CO $J=2-1$ observations showing unambiguously that the actual driving source of the HH 7–11 flow is SVS 13. Our observations also provide important information on the structure of this prototypical outflow.

2. Observations

The observations were carried out in March 1998 with the IRAM 5-antenna interferometer at Plateau de Bure. Three configurations of the array were used, with baselines extending up to 176 m. The dual-channel receivers were tuned to the CO $J=2-1$ and SiO $J=2-1$ frequencies. The SiO and continuum observations have been presented by Bachiller et al. (1998). Typical SSB system temperature was 300 K at the CO frequency. The correlator was configured to give a resolution of 3.3 km s^{-1} in a $\sim 400 \text{ km s}^{-1}$ wide interval. Phase calibration was achieved by observing 3C84, which is close in the sky to HH 7–11. Typical rms phase noise on the longest baselines was 30° . To correct for decorrelation due to the phase noise, the amplitude was also calibrated through the observations of 3C84, whose flux density was 2.6 Jy at 230.5 GHz. A mosaic of 10 fields was observed in order to cover the central region of the HH 7–11 outflow. Images were produced using natural weighting and cleaned with the GILDAS software. The clean beam is $2.4 \times 1.8''$ at the CO frequency. The continuum (see Bachiller et al. 1998) has been subtracted from the line maps.

Send offprint requests to: R. Bachiller

* Based on observations carried out with the IRAM Plateau de Bure Interferometer. IRAM is supported by INSU/CNRS (France), MPG (Germany) and IGN (Spain).

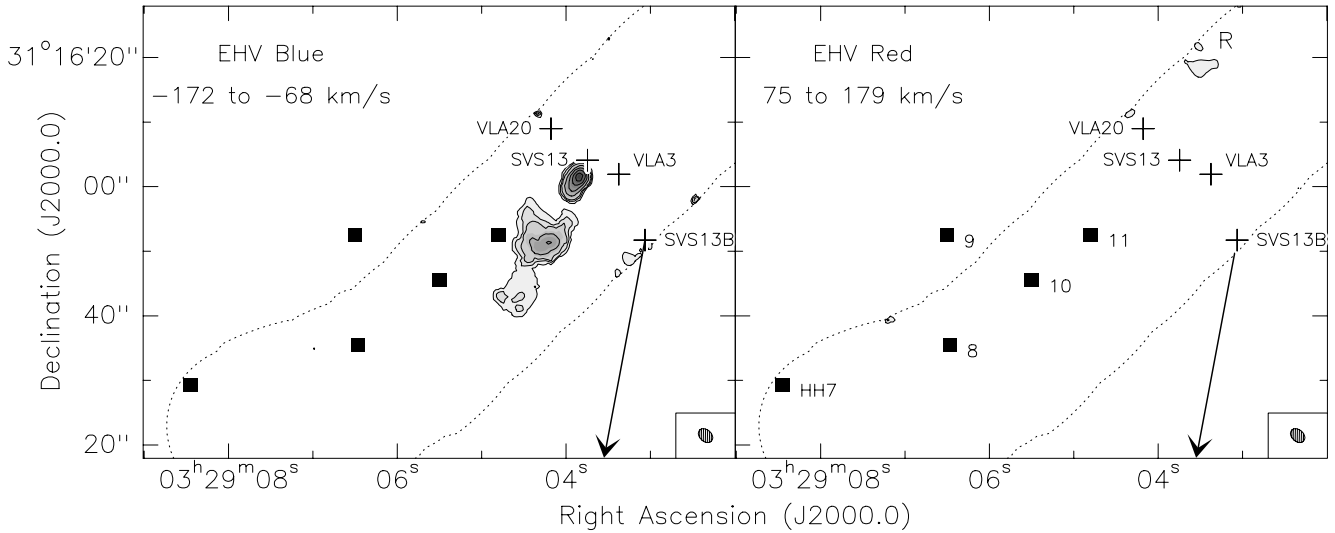


Fig. 1. CO $J=2-1$ line intensity around HH 7–11, integrated in extremely-high-velocity (EHV) intervals of 104 km s^{-1} width. The LSR velocity intervals are given in the top left corners. Contours are $1.4, 2.8, 4.2 \text{ Jy beam}^{-1} \text{ km s}^{-1}$, and then increase by $2.8 \text{ Jy beam}^{-1} \text{ km s}^{-1}$ step. Crosses mark the positions of VLA sources (Rodríguez et al. 1997, 1999), and of SVS 13 and SVS 13B (Bachiller et al. 1998). The arrow indicates the direction of the SVS 13B molecular outflow, and filled squares mark the positions of HH objects. The dotted line shows the limits of the observed region. The clean beam is also indicated.

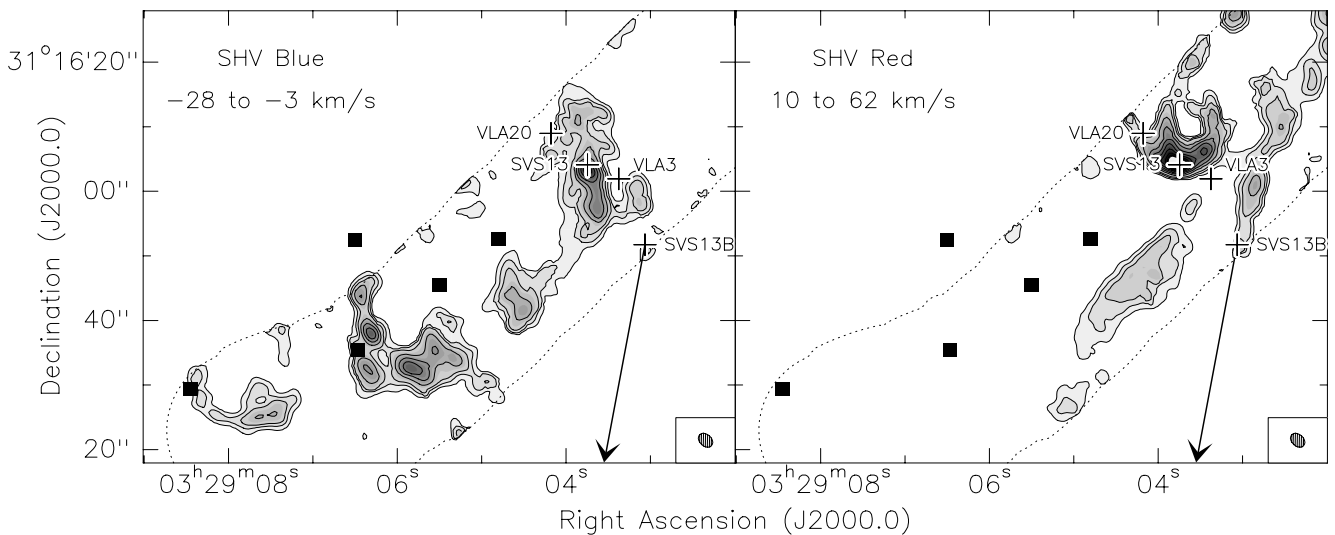


Fig. 2. CO $J=2-1$ intensity integrated in the standard-high-velocity (SHV) intervals which are indicated in the top left corner (velocities with respect to the LSR). Contours and symbols are as in Fig. 1.

3. Results

The interferometric CO $J=2-1$ images of the HH 7–11 vicinity are complex, reflecting the source crowding in the area. In order to summarize our results, we have divided the high-velocity emission into a limited number of velocity intervals. The most extreme velocities are presented in Fig. 1. Following Bachiller & Cernicharo (1990) we will refer to this component as the “extremely high velocity” (EHV) component, whereas the “standard high velocity” (SHV) component will designate the emission at lower velocities shown in Fig. 2. There is some emission at intermediate velocities exhibiting an intermediate behavior as compared to the maps discussed here.

3.1. EHV emission: the origin of HH 7–11

The EHV emission (Fig. 1) reveals an extended blueshifted structure, $\sim 25''$ long in the southeast direction from SVS 13, in good agreement with previous lower resolution maps (Bachiller & Cernicharo 1990, Masson et al. 1990). This jet-like feature consists of three well aligned clumps (“molecular bullets”) and emanates exactly from the position of SVS 13. As can be seen in the right panel of Fig. 1, the EHV redshifted emission reveals a small clump (marked “R” in the figure), $\sim 15''$ to the northwest from SVS 13. This bullet is well aligned with the blueshifted jet and is therefore likely to trace the redshifted, weaker lobe. The lower resolution maps already showed that the EHV red-

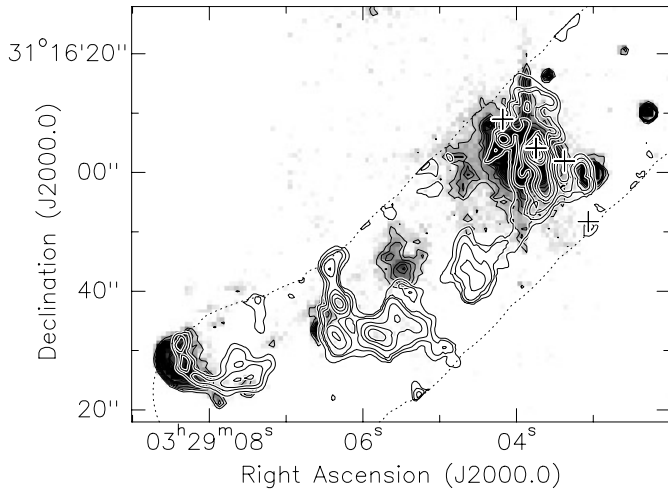


Fig. 3. Overlay of the K' emission (greyscale; from Hodapp 1994) and the SHV blueshifted CO $J=2-1$ emission (as in Fig. 2).

shifted emission is relatively weak in this area. There is however a strong peak $\sim 45''$ northwest from SVS 13, well beyond the area we imaged.

Bullet R is well detected over the noise level: its CO spectrum is a feature of $\sim 10 \text{ km s}^{-1}$ linewidth, centered at $V_{LSR} = 147 \text{ km s}^{-1}$. The LSR velocities of the three blueshifted CO bullets are -70 , -110 , and -150 km s^{-1} , when moving from SVS 13 to the southeast. An analysis of the extreme velocity SiO $J=2-1$ emission (not shown in Bachiller et al. 1998) shows that the first CO bullet also presents weak SiO emission in the same velocity range (i.e. up to -80 km s^{-1}). The SiO emission is compact ($< 4''$) and has an integrated intensity of 1.8 Jy km s^{-1} . The CO and SiO emission peaks are coincident within $0.5''$, and the CO/SiO integrated intensity ratio is ~ 25 . Unfortunately, because of backend limitations, the velocity coverage was insufficient to observe in SiO the two CO bullets more distant from SVS 13.

The typical sizes of the blueshifted CO bullets are $\sim 5''$, or 1500 AU at the assumed distance of 300 pc. The distance between successive CO peaks is $\sim 10''$ ($\sim 3000 \text{ AU}$). By assuming that the outflow is inclined by about 45° to the plane of the sky, we find that the time elapsed between successive ejection events is $\sim 100 \text{ yr}$. In this context, it is worth noting that SVS 13 itself also displays a high variability (Eisloffel et al. 1991), so it is tempting to suggest that the eruptions of the outflow are related to outbursts in the driving source.

The high spatial coincidence of the EHV jet extremity with SVS 13 (seen in both CO and SiO emission), and the lack of significant high-velocity CO emission from VLA3 and VLA20, strongly indicate that SVS 13 is the actual driving source of the HH 7–11 outflow.

3.2. SHV shell-like outflow

The SHV maps provide interesting information on the SVS 13B and SVS 13 outflows. The red map uncovers the northern lobe from SVS 13B, which is observed to be remarkably well aligned

with the southern blueshifted one (marked with an arrow in the figures; see Bachiller et al. 1998) and exhibits a similar high collimation. A SiO clump in this redshifted jet was reported by Bachiller et al. (1998), and coincides with the closest CO peak from SVS 13B.

Around HH 7–11, the SHV blueshifted emission forms a well developed arc, strongly suggesting it traces the southern flank of a shell surrounding the HH objects, with the apex at SVS 13. This SHV shell is coincident with the nebula seen in the optical and near-IR images (e.g. Hodapp & Ladd 1995), corresponding well to the cavity where the HH objects are formed. This is illustrated in Fig. 3 where the SHV emission is overlapped on the K' image of Hodapp (1994). The shell structure is not smooth, but appears broken in irregular clumps, which could be created as a result of the interaction with a strongly inhomogeneous medium, or by some instability process. Interestingly, there is a bow-shaped SHV structure near HH 7, probably indicating that this object marks an extremity of the cavity.

3.3. Changes in the direction of the outflow axis

The blueshifted EHV jet lies at P.A. 155° , i.e. on a different direction from that defined by the HH objects and the SHV shell (P.A. $\sim 130^\circ$). Since the EHV jet has probably been created by the most recent ejection phenomena (as indicated by its shorter kinematical timescale), we conclude that the outflow axis has moved by about $\sim 25^\circ$ toward the South from the period in which the SHV shell was created to the most recent ejection events. This change of the outflow axis could be due to precession in the ejection or to deflection of the outflow along its path. Recent observations of the H_2 shocks show that the proper motion vectors near HH 11 and HH 10 (the closest HH objects to SVS 13) have higher P.A. than those near HH 7 and HH 8 (Chrysostomou et al. 2000, their Fig. 1). The proper motions of HH 10–11 are very well aligned with the CO EHV jet and point to SVS 13. However, the proper motion vectors of HH 7–8 are better aligned with the SHV shell, and point to a position $\sim 20''$ south from SVS 13. Since a precession effect should preserve the vectors pointing towards SVS 13, the observed changes in the flow direction are probably due to the action of a force lateral to the outflow (e.g. dynamical or magnetic pressure, or collisions with ambient dense clumps).

4. Discussion

4.1. Evolutionary status of the HH 7–11/SVS 13 system

The data presented here provide important information on the structure of the HH 7–11 molecular outflow, and direct evidence on the identity of its driving source (SVS 13). It thus appears interesting to connect the characteristics of this well studied YSO with the properties of its outflow.

SVS 13 is a strong infrared source (Strom et al. 1976) of $85 L_\odot$ (based on Molinari et al. 1993, scaled to the distance assumed here) which experienced outbursts between 1988 and 1990 (Eisloffel et al. 1991) becoming even optically visible (Mauron & Thouvenot 1991). The source is associated with

a cm-wave source (named VLA4, Rodríguez et al. 1999) and it is embedded in a dusty disk or elongated envelope, of $\sim 1 M_{\odot}$, which is roughly perpendicular to the HH 7–11 chain (Bachiller et al. 1998). Briefly speaking, the characteristics of SVS 13 are those of a Class I object undergoing eruptions.

The HH 7–11 shell structure is similar to shells observed in both outflows from Class I sources (e.g. L 1551/IRS 5, Moriarty-Schieven et al. 1987) and outflows from Class 0 sources (e.g. L1527: Tamura et al. 1996; L1448: Bachiller et al. 1995). The L 1551 outflow is, however, spatially much more extended than HH 7–11, indicating that L 1551 is more evolved. Which is most notable in the case of SVS 13 -in principle a Class I object- is the presence of an EHV jet. Up to now such jets were believed to be characteristics of Class 0 sources such as L 1448-mm or IRAS 03282+3035 (Bachiller 1996, and references therein). In the HH 7–11 case, the chain of HH objects is more or less coincident with the axis of the SHV shell, in agreement with the idea that such Herbig Haro objects are tracing shocks in the central jet/wind.

The presence of strong SiO emission is also thought to be a property of very young outflows. The strongest component of SiO emission in the HH 7–11 vicinity arises from low velocity material, and seems therefore to be related to ambient gas rather than outflowing material (Bachiller et al. 1998, Lefloch et al. 1998, Codella et al. 1999). But as discussed in Sect. 3.1, there is also EHV SiO emission arising from at least one of the bullets in the jet. This SiO emission is quite weak compared to most Class 0 objects, which explains why it remained undetected in lower resolution observations, but it is significant.

In summary, although SVS 13 is a Class I object (based on its spectral energy distribution), its outflow presents some features of outflows from Class 0 sources. Furthermore, it is also remarkable that the nearby object SVS 13B, which is at a distance of only 4300 AU from SVS 13, is a bona-fide Class 0 object (Bachiller et al. 1998). At the view of these observational facts, we therefore suggest that SVS 13 is at the beginning of the Class I stage, and thus keeps some characteristics of the previous evolutionary stage. Another possibility is that SVS 13 is a relatively evolved Class 0 object which has already become optically visible due to a favourable viewing angle. We note that SVS 13 is about an order of magnitude more luminous than typical Class 0 sources, which hints at a more massive object. The persistence of Class 0 features in the outflow from the early Class I - or “mature” Class 0- source SVS 13 could therefore result from the faster evolution of the central star.

4.2. The nature of the VLA sources

The nature of the sources VLA 3 and VLA 20 remains uncertain. Although they are well detected at cm wavelengths (Rodríguez et al. 1997, 1999), their continuum mm-wave emission -if existent at all- is very low (Bachiller et al. 1998). The probability of finding two extragalactic sources so close to SVS 13 is negligible, and we should conclude that these objects are associated to the molecular cloud. The spectral index calculated from the

cm to the mm range is consistent with a flat spectrum, so one possibility could be that they are ionized knots in the outflows from other sources. However, both VLA 3 and VLA 20 are relatively well aligned with SVS 13 and SVS 13B on a line which is more or less perpendicular to the direction of the main outflows in the region (those from SVS 13 and SVS 13B), making this interpretation unlikely.

The upperlimit to the λ 1.3 mm flux of VLA 3 and VLA 20 is ~ 15 mJy which, under the assumptions used by Bachiller et al. (1998), indicates that a possible dusty circumstellar envelope or disk around these objects would have less than $0.05 M_{\odot}$ of mass. So, if they are young stars, their small amount of circumstellar mass would in principle indicate that they are relatively evolved. Moreover, in such a case, they should have very low luminosities, since -in spite of their low circumstellar extinction- they are not seen in the near-infrared. More observations are needed to unveil the nature of these enigmatic VLA sources. In case they were confirmed to be stellar objects associated to the molecular cloud, it will be extremely interesting to estimate their masses and to study their evolutionary status.

Acknowledgements. We remain obliged to the IRAM staff at Plateau de Bure for help with the observations, and in particular to those staff members who lost their lives in two tragic accidents in 1999. RB and MT acknowledge support from Spanish DGES grant PB96-104.

References

- Anglada G., Rodríguez L.F., Torrelles J.M., 2000, *ApJ*, in press
 Aspin C., Sandell G., Russel A.P.G., 1994, *A&AS* 106, 165
 Bachiller R., 1996, *ARA&A* 34, 111
 Bachiller R., Cernicharo J., 1990, *A&A* 239, 276
 Bachiller R., Guilloteau S., Dutrey A., et al. 1995, *A&A* 299, 857
 Bachiller R., Guilloteau S., Gueth F., et al. 1998, *A&A* 339, L49
 Bally J., Devine D., Reipurth B., 1996, *ApJ* 473, L49
 Cernis K., 1990, *ApSS* 166, 315
 Chrysostomou A., Hobson J., Davis C.J., et al. 2000, *MNRAS* 314, 229
 Codella C., Bachiller R., Reipurth B., 1999, *A&A* 343, 585
 Eislöffel J., Günther E., Hessman F.V. et al. 1991 *ApJ* 383, L19
 Herbig G.H., Jones B.F., 1983, *AJ* 88, 1040
 Hodapp K.-W., 1994, *ApJS* 64, 615
 Hodapp K.-W., Ladd E.F., 1995, *ApJ* 453, 715
 Knee L.B.G., Sandell G., 2000, *A&A*, in press
 Lefloch B., Castets A., Cernicharo J., et al. 1998, *ApJ* 504, L109
 Lizano S., Heiles C., Rodríguez, L.F., et al. 1988, *ApJ* 328, 763
 Masson C.R., Mundy L.G., Keene J., 1990, *ApJ* 357, L25
 Maunon N., Thouvenot E., 1991, *IAU Circ.*, 5261
 Molinari S., Liseau R., Lorenzetti D., 1993, *A&AS* 101, 59
 Moriarty-Schieven G.H., Snell R.L., Strom S.E., et al. 1987, *ApJ* 319, 742
 Rodríguez L.F., Lizano S., Cantó J., et al. 1990, *ApJ* 365, 261
 Rodríguez L.F., Anglada G., Curiel S., 1997, *ApJ* 480, L125
 Rodríguez L.F., Anglada G., Curiel S., 1999, *ApJ* 515, 427
 Snell R.L., Edwards S. 1981, *ApJ* 251, 103
 Strom, S.E., Vrba, F.J., Strom, K.M. 1976, *AJ* 81, 314
 Tamura, M., Ohashi, N., Hirano, N., et al. 1996, *AJ* 112, 2076